Available online at www.sciencedirect.com

ScienceDirect

Energy and Buildings 40 (2008) 157–167

ENERGY and BUILDINGS

www.elsevier.com/locate/enbuild

Estimation of non-linear continuous time models for the heat exchange dynamics of building integrated photovoltaic modules

M.J. Jiménez [a,*], H. Madsen [b], J.J. Bloem [c], B. Dammann [b]

[a] Department of Energy, Energy Efficiency in Buildings Unit, CIEMAT, Av. Complutense 22, E-28040, Madrid, Spain

[b] Informatics and Mathematical Modelling, Technical University of Denmark, Building 321, DK-2800 Lyngby, Denmark

[c] European Commission, Joint Research Centre, Building 45, I-21020 Ispra, Italy

Received 10 October 2006; received in revised form 15 February 2007; accepted 19 February 2007

Abstract

This paper focuses on a method for linear or non-linear continuous time modelling of physical systems using discrete time data. This approach facilitates a more appropriate modelling of more realistic non-linear systems. Particularly concerning advanced building components, convective and radiative heat interchanges are non-linear effects and represent significant contributions in a variety of components such as photovoltaic integrated façades or roofs and those using these effects as passive cooling strategies, etc. Since models are approximations of the physical system and data is encumbered with measurement errors it is also argued that it is important to consider stochastic models.

More specifically this paper advocates for using continuous–discrete stochastic state space models in the form of non-linear partially observed stochastic differential equations (SDE's)—with measurement noise for modelling dynamic systems in continuous time using discrete time data. First of all the proposed method provides a method for modelling non-linear systems with partially observed states. The approach allows parameters to be estimated from experimental data in a *prediction error* (PE) setting, which gives less biased and more reproducible results in the presence of significant process noise than the more commonly used *output error* (OE) setting. To facilitate the use of continuous–discrete stochastic state space models, a PE estimation scheme that features *maximum likelihood* (ML) and *maximum a posteriori* (MAP) estimation is presented along with a software implementation.

As a case study, the modelling of the thermal characteristics of a building integrated PV component is considered. The EC-JRC Ispra has made experimental data available. Both linear and non-linear models are identified. It is shown that a description of the non-linear heat transfer is essential. The resulting model is a non-linear first order stochastic differential equation for the heat transfer of the PV component.

Keywords: Continuous time systems; Stochastic modelling; Non-linear systems; Parameter estimation; Prediction error methods; Maximum likelihood estimators; Extended Kalman filters; Software tools; Parallel computation; PV element; Thermal analysis

1. Introduction

Since the pioneering work of [1] and [2] modelling of dynamics systems based on stochastic differential equations (SDE's) has received limited attention. This is evident from a series of review papers on the state of the art of identification of continuous time models [3–5]. It is, however, the opinion of the authors of the present paper that the topic deserves much more attention, because SDE's, when used in the context of a continuous–discrete stochastic state space model, constitute a very natural framework for modelling realistic physical systems, since non-linear model structures and prior physical knowledge can be used.

Continuous–discrete stochastic state space models consist of a set of SDE's describing the dynamics of the system in continuous time and a set of discrete time measurement equations. This model type very correctly reflects the real world of most dynamic systems, where system dynamics are inherently continuous and at the same time subject to random effects, whereas, measurements are inherently discrete. Furthermore, many, especially physical, chemical and biological, systems have a large number of state variables, of which usually only a subset can be measured, and this is easily reflected by models of this type as well. The particular structure of continuous–discrete stochastic state space models also implies that they can be easily derived from first principles, that

* Corresponding author. Tel.: +34 950 387922; fax: +34 950 365015.
E-mail address: Mjose.jimenez@psa.es (M.J. Jiménez).

0378-7788/$ – see front matter © 2007 Elsevier B.V. All rights reserved.
doi:10.1016/j.enbuild.2007.02.026

Nomenclature

A	total surface area of the PV module
c_p	specific heat for air
h_c	convective heat transfer coefficient
I_v	vertical global irradiance
p	fraction of energy to air in the cavity from PV module
S	section of the outlet tube
T	temperature of PV module
ΔT	air temperature difference between inlet and outlet
T_a	ambient air temperature
T_{rad}	mean radiant temperature
w_{gap}	air velocity in outlet tube

Greek letters

α	absorptance of the PV module
ϵ_{pv1}	emissivity—exterior surface of PV module
ϵ_{pv2}	emissivity—interior surface of PV module
ϵ_w	emissivity of the wood surface
σ	Stefan–Boltzman constant
ρ	air density

physical insights and other prior information can be incorporated directly, and owing to the continuous time formulation the parameters of the models are more easily given a physical interpretation.

A final advantage of continuous–discrete stochastic state space models is that they allow for a decomposition of the noise affecting the system into a process noise term and a measurement noise term. As a consequence of this *prediction error decomposition*, unknown parameters of such models can be estimated from experimental data in a *prediction error* (PE) setting as opposed to the more commonly used *output error* (OE) setting, which gives more biased and less reproducible results in the presence of significant process noise, because random effects are absorbed into the parameter estimates. Furthermore, PE estimation allows for subsequent application of a number of powerful statistical tools to provide indications for possible improvements to the structure of the model. In particular, estimates of the parameters of the diffusion term can be used to assess the quality of a model and to pinpoint model deficiencies in order to subsequently uncover their structural origin [6].

The focus of the present paper is on estimation of unknown parameters in continuous time models based on discrete time data. The method described in this paper can be considered as an extension to the methods described in [7,8]. These methods have been widely used in estimating models of the heat dynamics of buildings and HVAC components [9]. In the previous work only linear models were considered, and only a single data set could be applied. The updated approach presented in this paper allow for both non-linear models and for the use of multiple data sets. For example, this updated approach allow for a direct use of physical laws describing the non-linear heat transfer by radiation and convection. It is the purpose of the present approach to somehow fill the gap between detailed non-linear physical modelling and more simple black-box oriented statistical modelling. The combined approach is often called a grey box approach [10]. For a detailed outline of the method is we refer to [11,12], or [10].

The primary aim of the paper is to give an outline of an efficient and flexible scheme for performing the estimation for continuous–discrete stochastic state space models and briefly mention a software implementation of this scheme. A secondary aim of the paper is to demonstrate the use of this approach for modelling the heat dynamics of a PV-component. This case study turns out to lead to rather simple dynamic models where it is crucial to take the non-linearities into account.

The remainder of the paper is organized as follows: in Section 2, the estimation methodology is outlined, and in Section 4, the software implementation is described. In Section 6, the modelling of the PV component is considered, and in Section 7, the results are discussed. Finally, in Section 8, the conclusions of the paper are given.

2. Estimation methodology

This section contains a condensed outline of a PE estimation scheme for continuous–discrete time stochastic state space models. A detailed outline of the scheme is given by [11] or [10].

2.1. Model structure

In the general case, the continuous–discrete stochastic state space model is a model that consists of a set of non-linear discretely, partially observed SDE's with measurement noise, i.e.,

$$d\boldsymbol{x}_t = \boldsymbol{f}(\boldsymbol{x}_t, \boldsymbol{u}_t, t, \boldsymbol{\theta})\, dt + \boldsymbol{\sigma}(\boldsymbol{u}_t, t, \boldsymbol{\theta})\, d\boldsymbol{\omega}_t \tag{1}$$

$$\boldsymbol{y}_k = \boldsymbol{h}(\boldsymbol{x}_k, \boldsymbol{u}_k, t_k, \boldsymbol{\theta}) + \boldsymbol{e}_k \tag{2}$$

where $t \in \mathbb{R}$ is the time variable; $\boldsymbol{x}_t \in \mathcal{X} \subset \mathbb{R}^n$ is a vector of state variables; $\boldsymbol{u}_t \in \mathcal{U} \subset \mathbb{R}^m$ is a vector of input variables; $\boldsymbol{y}_k \in \mathcal{Y} \subset \mathbb{R}^l$ is a vector of output variables; $\boldsymbol{\theta} \in \Theta \subset \mathbb{R}^p$ is a vector of (possibly unknown) parameters; $\boldsymbol{f}(\cdot) \in \mathbb{R}^n$, $\boldsymbol{\sigma}(\cdot) \in \mathbb{R}^{n \times n}$ and $\boldsymbol{h}(\cdot) \in \mathbb{R}^l$ are non-linear functions; $\{\boldsymbol{\omega}_t\}$ is an n-dimensional standard Wiener process; $\{\boldsymbol{e}_k\}$ is an l-dimensional white noise process with $\boldsymbol{e}_k \in N(\boldsymbol{0}, \boldsymbol{S}(\boldsymbol{u}_k, t_k, \boldsymbol{\theta}))$.

SDE's may be interpreted both in the sense of Stratonovich and in the sense of Itô, but since the Stratonovich interpretation is less suitable for parameter estimation [1,2], the Itô interpretation is adapted. Furthermore, the diffusion term in (1) is assumed to be independent of the state variables, because this renders parameter estimation more feasible.

2.2. Parameter estimation

The solution to (1) is a Markov process and an estimation scheme based on probabilistic methods can therefore be applied to estimate the unknown parameters of the model in (1) and (2), e.g. *maximum likelihood* (ML) or *maximum a posteriori* (MAP), where the latter can be applied if prior information about the parameters is available. Let:

$$\mathbf{Y} = [\mathcal{Y}^1_{N_1}, \mathcal{Y}^2_{N_2}, \ldots, \mathcal{Y}^i_{N_i}, \ldots, \mathcal{Y}^S_{N_S}] \tag{3}$$

be a set of S stochastically independent sequences of consecutive measurements, where:

$$\mathcal{Y}^i_{N_i} = [\boldsymbol{y}^i_{N_i}, \ldots, \boldsymbol{y}^i_k, \ldots, \boldsymbol{y}^i_1, \boldsymbol{y}^i_0] \tag{4}$$

and let $p(\boldsymbol{\theta})$ be a prior probability density function for the parameters. In the general case, point estimates of the parameters in (1) and (2) can then be found as the parameters $\boldsymbol{\theta}$ that maximize the posterior probability density function:

$$p(\boldsymbol{\theta}|\mathbf{Y}) \propto \left(\prod_{i=1}^{S} p(\mathcal{Y}^i_{N_i}|\boldsymbol{\theta})\right) p(\boldsymbol{\theta}) \tag{5}$$

or equivalently:

$$p(\boldsymbol{\theta}|\mathbf{Y}) \propto \left(\prod_{i=1}^{S}\left(\prod_{k=1}^{N_i} p(\boldsymbol{y}^i_k|\mathcal{Y}^i_{k-1}, \boldsymbol{\theta})\right) p(\boldsymbol{y}^i_0|\boldsymbol{\theta})\right) p(\boldsymbol{\theta}) \tag{6}$$

where the rule $P(A \cap B) = P(A|B)P(B)$ has been applied in a successive manner to form products of conditional probability density functions.

In order to obtain an exact evaluation of the posterior probability density function in (6), the initial probability density functions $p(\boldsymbol{y}^i_0|\boldsymbol{\theta})$, $i = 1, \ldots, S$, must be known and all subsequent conditional probability density functions must be determined by successive prediction and updating [1]. In practice this approach is computationally infeasible and an alternative is therefore needed. [3] has a review of the state of the art with respect to parameter estimation in discretely observed SDE's, which shows that for models of the type in (1) and (2) only methods based on approximate non-linear filters provide a computationally feasible solution to the problem. However, since the diffusion term in (1) has been assumed to be independent of the state variables, a much simpler alternative can be applied here.

More specifically, since the SDE's in (1) are driven by a Wiener process, and since increments of a Wiener process are Gaussian, it is reasonable to assume, under some regularity conditions, that the conditional probability density functions can be well approximated by Gaussian densities, which means that a method based on the extended Kalman filter (EKF) can be applied. The Gaussian density is completely characterized by its mean and covariance, so by introducing:

$$\hat{\boldsymbol{y}}^i_{k|k-1} = E\{\boldsymbol{y}^i_k|\mathcal{Y}^i_{k-1}, \boldsymbol{\theta}\} \tag{7}$$

$$\boldsymbol{R}^i_{k|k-1} = V\{\boldsymbol{y}^i_k|\mathcal{Y}^i_{k-1}, \boldsymbol{\theta}\} \tag{8}$$

$$\boldsymbol{\epsilon}^i_k = \boldsymbol{y}^i_k - \hat{\boldsymbol{y}}^i_{k|k-1} \tag{9}$$

and by further assuming that the prior probability density function for the parameters is Gaussian as well, and therefore, also introducing:

$$\boldsymbol{\mu}_{\boldsymbol{\theta}} = E\{\boldsymbol{\theta}\} \tag{10}$$

$$\Sigma_{\boldsymbol{\theta}} = V\{\boldsymbol{\theta}\} \tag{11}$$

$$\boldsymbol{\epsilon}_{\boldsymbol{\theta}} = \boldsymbol{\theta} - \boldsymbol{\mu}_{\boldsymbol{\theta}} \tag{12}$$

the posterior probability density function becomes:

$$p(\boldsymbol{\theta}|\mathbf{Y}) \propto \left(\prod_{i=1}^{S}\left(\prod_{k=1}^{Ni} \frac{\exp(-\frac{1}{2}(\boldsymbol{\varepsilon}^i_k)^T(\boldsymbol{R}^i_{k|k-1})^{-1}\boldsymbol{\varepsilon}^i_k)}{\sqrt{det(\boldsymbol{R}^i_{k|k-1})(\sqrt{2\pi})^l}}\right) p(\boldsymbol{y}^i_0|\theta)\right) \times \frac{\exp(-\frac{1}{2}\boldsymbol{\varepsilon}^T_\theta \Sigma^{-1}_\theta \boldsymbol{\varepsilon}_\theta)}{\sqrt{det(\Sigma_\theta)(\sqrt{2\pi})^p}} \tag{13}$$

The parameter estimates can now be determined by further conditioning on the initial conditions:

$$\mathbf{y}_0 = [\boldsymbol{y}^1_0, \boldsymbol{y}^2_0, \ldots, \boldsymbol{y}^i_0, \ldots, \boldsymbol{y}^S_0] \tag{14}$$

and applying non-linear optimisation to find the minimum of the negative logarithm of the resulting posterior probability density function, i.e.,

$$\hat{\boldsymbol{\theta}} = \arg\min_{\boldsymbol{\theta} \in \Theta}\{-\ln(p(\boldsymbol{\theta}|\mathbf{Y}, \mathbf{y}_0))\} \tag{15}$$

In the general case the estimation method implied by (15) is MAP, but, if no prior information about the parameters is available, it reduces to ML.

In either case, the innovations $\boldsymbol{\epsilon}^i_k$ and their covariances $\boldsymbol{R}^i_{k|k-1}$ can be computed recursively by means of the EKF for each set of parameters $\boldsymbol{\theta}$ in the optimisation. More specifically, the EKF consists of the output *prediction* equations:

$$\hat{\boldsymbol{y}}^i_{k|k-1} = \boldsymbol{h}(\hat{\boldsymbol{x}}^i_{k|k-1}, \boldsymbol{u}^i_k, t^i_k, \boldsymbol{\theta}) \tag{16}$$

$$\boldsymbol{R}^i_{k|k-1} = \boldsymbol{C}\boldsymbol{P}^i_{k|k-1}\boldsymbol{C}^T + \boldsymbol{S} \tag{17}$$

the *innovation* equation:

$$\boldsymbol{\epsilon}^i_k = \boldsymbol{y}^i_k - \hat{\boldsymbol{y}}^i_{k|k-1} \tag{18}$$

the Kalman *gain* equation:

$$\boldsymbol{K}^i_k = \boldsymbol{P}^i_{k|k-1}\boldsymbol{C}^T(\boldsymbol{R}^i_{k|k-1})^{-1} \tag{19}$$

the *updating* equations:

$$\hat{\boldsymbol{x}}^i_{k|k} = \hat{\boldsymbol{x}}^i_{k|k-1} + \boldsymbol{K}^i_k\boldsymbol{\epsilon}^i_k \tag{20}$$

$$\boldsymbol{P}^i_{k|k} = \boldsymbol{P}^i_{k|k-1} - \boldsymbol{K}^i_k\boldsymbol{R}^i_{k|k-1}(\boldsymbol{K}^i_k)^T \tag{21}$$

where

$$\hat{\boldsymbol{x}}^i_{k|k} = E\{\boldsymbol{x}^i_k|\mathcal{Y}^i_k, \boldsymbol{\theta}\} \tag{22}$$

$$\boldsymbol{P}^i_{k|k} = V\{\boldsymbol{x}^i_k|\mathcal{Y}^i_k, \boldsymbol{\theta}\} \tag{23}$$

i.e. the conditional mean and covariance of the state vector.

The state *prediction* equations:

$$\frac{d\hat{\boldsymbol{x}}^i_{t|k}}{dt} = \boldsymbol{f}(\hat{\boldsymbol{x}}^i_{t|k}, \boldsymbol{u}^i_t, t, \boldsymbol{\theta}) \tag{24}$$

$$\frac{d\boldsymbol{P}^i_{t|k}}{dt} = \boldsymbol{A}\boldsymbol{P}^i_{t|k} + \boldsymbol{P}^i_{t|k}\boldsymbol{A}^T + \boldsymbol{\sigma}\boldsymbol{\sigma}^T \tag{25}$$

which are solved for $t \in [t^i_k, t^i_{k+1}[$. In the above equations, the following notation has been applied:

$$\boldsymbol{A} = \left.\frac{\partial \boldsymbol{f}}{\partial \boldsymbol{x}_t}\right|_{\hat{\boldsymbol{x}}^i_{k|k-1}, \boldsymbol{u}^i_k, t^i_k}, \quad \boldsymbol{C} = \left.\frac{\partial \boldsymbol{h}}{\partial \boldsymbol{x}_t}\right|_{\hat{\boldsymbol{x}}^i_{k|k-1}, \boldsymbol{u}^i_k, t^i_k} \quad \boldsymbol{\sigma} = \boldsymbol{\sigma}(\boldsymbol{u}^i_k, t^i_k, \boldsymbol{\theta}),$$
$$\boldsymbol{S} = \boldsymbol{S}(\boldsymbol{u}^i_k, t^i_k, \boldsymbol{\theta})$$

Initial conditions for the EKF are $\hat{\boldsymbol{x}}^i_{t|t_0} = \boldsymbol{x}^i_0$ and $\boldsymbol{P}^i_{t|t_0} = \boldsymbol{P}^i_0$, which can either be prespecified or estimated as a part of the overall problem.

The EKF is sensitive to non-linear effects and the approximate solution obtained by solving (24) and (25) may be too crude [1], so in order to obtain a better approximation, the time interval $[t^i_k, t^i_{k+1}[$ is sub-sampled, i.e. $[t^i_k, \ldots, t^i_j, \ldots, t^i_{k+1}[$, and the equations are linearized at each sub-sampling instant. This way the numerical solution of (24) and (25) can also be simplified by applying the analytical solutions to the corresponding linearized propagation equations:

$$\frac{d\hat{\boldsymbol{x}}^i_{t|j}}{dt} = \boldsymbol{f}_0 + \boldsymbol{A}(\hat{\boldsymbol{x}}^i_t - \hat{\boldsymbol{x}}^i_j) + \boldsymbol{B}(\boldsymbol{u}^i_t - \boldsymbol{u}^i_j) \tag{26}$$

$$\frac{d\boldsymbol{P}^i_{t|j}}{dt} = \boldsymbol{A}\boldsymbol{P}^i_{t|j} + \boldsymbol{P}^i_{t|j}\boldsymbol{A}^T + \boldsymbol{\sigma}\boldsymbol{\sigma}^T \tag{27}$$

for $t \in [t^i_j, t^i_{j+1}[$, where the notation:

$$\boldsymbol{A} = \left.\frac{\partial \boldsymbol{f}}{\partial \boldsymbol{x}_t}\right|_{\hat{\boldsymbol{x}}^i_{j|j-1}, \boldsymbol{u}^i_j, t^i_j}, \quad \boldsymbol{B} = \left.\frac{\partial \boldsymbol{f}}{\partial \boldsymbol{u}_t}\right|_{\hat{\boldsymbol{x}}^i_{j|j-1}, \boldsymbol{u}^i_j, t^i_j}$$
$$\boldsymbol{f}_0 = \boldsymbol{f}(\hat{\boldsymbol{x}}^i_{j|j-1}, \boldsymbol{u}^i_j, t^i_j, \boldsymbol{\theta}), \quad \boldsymbol{\sigma} = \boldsymbol{\sigma}(\boldsymbol{u}^i_j, t^i_j, \boldsymbol{\theta})$$

has been applied. The analytical solutions are:

$$\hat{\boldsymbol{x}}^i_{j+1|j} = \hat{\boldsymbol{x}}^i_{j|j} + \boldsymbol{A}^{-1}(\Phi_s - \boldsymbol{I})\boldsymbol{f}_0 + (\boldsymbol{A}^{-1}(\Phi_s - \boldsymbol{I}) - \boldsymbol{I}\tau_s)\boldsymbol{A}^{-1}\boldsymbol{B}\boldsymbol{\alpha} \tag{28}$$

$$\boldsymbol{P}^i_{j+1|j} = \Phi_s\boldsymbol{P}^i_{j|j}\Phi_s^T + \int_0^{\tau_s} e^{\boldsymbol{A}s}\boldsymbol{\sigma}\boldsymbol{\sigma}^T e^{\boldsymbol{A}^T s}\,ds \tag{29}$$

where $\tau_s = t^i_{j+1} - t^i_j$ and $\Phi_s = e^{\boldsymbol{A}\tau_s}$, and where

$$\boldsymbol{\alpha} = \frac{\boldsymbol{u}^i_{j+1} - \boldsymbol{u}^i_j}{t^i_{j+1} - t^i_j} \tag{30}$$

has been introduced to allow assumption of either *zero order hold* ($\boldsymbol{\alpha} = \boldsymbol{0}$) or *first order hold* ($\boldsymbol{\alpha} \neq \boldsymbol{0}$) on the inputs between sampling instants. More details, e.g. about computing the matrix exponential $\Phi_s = e^{\boldsymbol{A}\tau_s}$, are given by [10].

The approach described above relies on a number of assumptions and approximations, which may be critical. Methods exist, however, for testing whether or not the identified model consistently describes the estimation data [13], as also briefly described in the next sections.

2.3. Uncertainty of parameter estimates

Essential outputs of any sound statistical parameter estimation scheme include an assessment of the uncertainty of the estimates. An estimate of the uncertainty of the parameter estimates can be obtained by using the fact that by the central limit theorem the estimator in (15) is asymptotically Gaussian with mean $\boldsymbol{\theta}$ and covariance matrix:

$$\Sigma_{\hat{\boldsymbol{\theta}}} = \boldsymbol{H}^{-1} \tag{31}$$

where the matrix $\boldsymbol{H}$ is given by the elements:

$$h_{ij} = -E\left\{\frac{\partial^2}{\partial\theta_i\partial\theta_j}\ln\left(p(\boldsymbol{\theta}|\mathbf{Y}, \mathbf{y}_0)\right)\right\}$$

for $i, j = 1, \ldots, p$, and where an approximation to $\boldsymbol{H}$ can be obtained from the elements:

$$h_{ij} \approx -\left.\left(\frac{\partial^2}{\partial\theta_i\partial\theta_j}\ln\left(p(\boldsymbol{\theta}|\mathbf{Y}, \mathbf{y}_0)\right)\right)\right|_{\boldsymbol{\theta}=\hat{\boldsymbol{\theta}}}$$

for $i, j = 1, \ldots, p$, which is the Hessian at the minimum of the objective function. A measure of the uncertainty of the individual estimates can be obtained by decomposing the covariance matrix:

$$\Sigma_{\hat{\boldsymbol{\theta}}} = \boldsymbol{\sigma}_{\hat{\boldsymbol{\theta}}}\boldsymbol{R}\boldsymbol{\sigma}_{\hat{\boldsymbol{\theta}}} \tag{32}$$

into $\boldsymbol{\sigma}_{\hat{\boldsymbol{\theta}}}$, which is a diagonal matrix of the standard deviations of the parameter estimates, and $\boldsymbol{R}$, which is the corresponding correlation matrix.

The uncertainty information thus obtained can subsequently be applied to perform tests of various hypotheses, e.g. to determine the significance of the individual parameters through *t*-tests, as described in the next section.

3. Statistical tests

The asymptotic Gaussianity of the estimator in (15) also allows *t*-tests to be performed to test the hypothesis:

$$H_0: \quad \theta_j = 0 \tag{33}$$

against the alternative:

$$H_1: \quad \theta_j \neq 0 \tag{34}$$

i.e. to test whether a given parameter θ_j is marginally insignificant or not. The test quantity is the value of the parameter estimate divided by the standard deviation of the estimate, and under H_0 this quantity is asymptotically *t*-distributed with a number of degrees of freedom DF that equals the total number of observations minus the number of estimated parameters, i.e.

$$z^t(\hat{\theta}_j) = \frac{\hat{\theta}_j}{\sigma_{\hat{\theta}_j}} \in t(\mathrm{DF}) = t\left(\left(\sum_{i=1}^{S}\sum_{k=1}^{N_i} l\right) - p\right) \tag{35}$$

where, if there are missing observations in $\mathbf{y}_k^i$ for some i and some k, l is replaced with the appropriate value of $\bar{l}$. To facilitate these tests, $z^t(\hat{\theta}_j),\ j = 1, \ldots, p$, are computed along with the probabilities:

$$P(t < -|z^t(\hat{\theta}_j)| \wedge t > |z^t(\hat{\theta}_j)|), \quad j = 1, \ldots, p \tag{36}$$

More details about the statistical tests can be found in [14] and [12].

4. Software implementation

The parameter estimation scheme presented in Section 2 has been implemented in a computer program called CTSM. This program is available for both Linux, Solaris and Windows platforms [10], and within its graphical user interface (GUI) unknown parameters of models of the kind in (1) and (2) can be estimated using the methods presented in Section 2. Once a model structure has been set up within the GUI, the program analyzes the model equations to determine the symbolic names of the parameters and displays them to allow the user to specify which parameters to fix, which to estimate, and how each parameter should be estimated (ML or MAP). After specifying which data sets to use, the program then determines the parameter estimates and computes the uncertainty information described in Section 2. The program also provides features to deal with occasional outliers and missing observations, and on Solaris systems the program supports shared memory parallelization to alleviate the extensive computational load often associated with estimation of parameters in continuous–discrete stochastic state space models.

5. Model validation

After having estimated the parameters of a model and verified that the estimated parameters are significant, the next step is the model validation. The purpose of the model validation step is to verify statistically whether the model adequately describes the considered system, or more precisely the observed data.

Some of the basic assumptions used in formulating the model are that the system error is a Wiener process and the measurement error is a Gaussian white noise sequence. Since integration of the Wiener process over two subsequent (non-overlapping) time intervals leads to two independent random variables, the sequence of one-step prediction error for an adequate model must be a sequence of independent random variables. This can be tested by using some test for white noise, as outlined in the following.

If the residuals are not white noise this implies that the residuals contains autocorrelation that can be used for improving the model and the predictions. A plot of the autocorrelation function or the partial autocorrelation function for such residuals may indicate how to improve the model. If, for instance, the partial autocorrelation function contains a significant coefficient in lag one only, this implies that yet another state variable has to be introduced.

Let us briefly introduce the concept of autocorrelation functions. If the process is stationary then the autocorrelation function is only a function of the time difference $t_2 - t_1$. Denoting the time difference (or time lag) by k, we have the *autocovariance function* for a stationary process $X(t)$:

$$\gamma(k) = \mathrm{Cov}[X(t), X(t+k)], \tag{37}$$

and the *autocorrelation function*:

$$\rho(k) = \frac{\gamma(k)}{\gamma(0)} = \frac{\gamma(\tau)}{\sigma_X^2}, \tag{38}$$

where $\sigma_X^2(t)$ is the variance of the process. Please note that $\rho(0) = 1$.

For a white noise process the autocorrelation function is

$$\rho(k) = \begin{cases} 1 & k = 0 \\ 0 & k = \pm 1, \pm 2, \ldots \end{cases} \tag{39}$$

The name white noise is due to the fact, that the spectral density for the process is constant.

Given a time series of lenght N, *an estimate* of the *autocovariance function* is obtained by

$$\mathrm{C}(k) = \mathrm{C}(k) = \frac{1}{N} \sum_{t=1}^{N-|k|} (Y_t - \bar{Y})(Y_{t+|k|} - \bar{Y}) \tag{40}$$

for $|k| = 0, 1, \ldots, N-1$. Furthermore, $\bar{Y} = (\sum_{t=1}^{N} Y_t)/N$.

Based on the *estimated autocovariance function* we find the *estimated autocorrelation function* as

$$\hat{\rho}(k) = r_k = \frac{\mathrm{C}(k)}{\mathrm{C}(0)}, \tag{41}$$

Asymptotically (for $N \to \infty$) both the estimates of the autocovariance and the autocorrelation will be normally distributed; but the mean valued and the variance are in general dependent on the theoretical autocovariance function, and thus, in practice impossible to calculate. Albeit, if the process or the sequence of residuals is white noise we have that

$$\mathrm{e}[\hat{\rho}(k)] \simeq 0; \quad k \neq 0, \tag{42}$$

$$V[\hat{\rho}(k)] \simeq \frac{1}{N}; \quad k \neq 0. \tag{43}$$

Furthermore, is $\hat{\rho}(k)$ asymptotically normally distributed.

Based on the asymptotical normality and under the hypothesis of white noise, one can make *an* (*approximative*) 95% *confidence interval* as $\pm 2\sqrt{1/N}$. When judging several lag values one have to bear in mind, that even if the process is white noise, about 5% of the values will be outside this confidence interval.

6. Case study: modelling of a PV component

6.1. Objective

The objective of this study is to illustrate the possibility for estimating parameters in continuous time linear and non-linear stochastic models using the method outlined in this paper.

Further, we shall focus on the use of the proposed statistical approaches for model validation.

As a case study we shall consider the modeling the thermal dynamics of a PV test reference module mounted in a test reference environment for building integration. Ultimately, the purpose of the experimental setup is to investigate the heat transfer of a PV device in a typical built environment.

A correct modelling is hampered by the lack of detailed experimental data. To overcome that problem a specific experiment was designed for ventilated photovoltaic facades. Four poly-crystalline PV modules were selected and were tested under different real weather conditions. The ventilated airflow in the gap behind the PV module and the radiative exchange between the PV module and the facing wall was changed also. The result of the experiments was a series of well-controlled data that contained information to study in particular the convective and radiative heat exchange energy flows.

6.2. Introduction to building integrated PV applications

At the European Commission DG, Joint Research Centre, the European Solar Test Installation is situated which activities are to certify PV modules for the European market and to perform supporting research for standardisation. At present the international standard [15] describes the electrical and mechanical performance tests for PV modules aimed for optimised free rack conditions. About 85% of the global PV market concerns mono- and poly-crystalline Silicon modules. The electrical performance depends largely on the PV module operating temperature. More and more PV installations are designed for built environmental conditions like facades and roofs in which case the PV module temperature depends on the boundary conditions such as adjacent construction and airflow. At present, international standard organisations are developing standards that will include the impact of the built environment on the performance of PV modules. It is therefore that at the JRC a reference environment has been designed to study in detail the dynamic heat exchange of PV modules in the built environment. Building designers are interested in performance under operating conditions for a typical climate, season and specific location taking into account the energy use of their design. Integration of PV in the building envelope implies that they have to take into account electrical energy production, but also thermal (avoid overheating in summer) and comfort (daylight, ventilation and quality of air) aspects. A further consideration is that building designers need performance indicators based on climatic variables: ambient temperature, solar radiation, wind velocity and site dependent data such as obstructions giving possible shading problems.

The technical data provided by the PV industry is based on standardised measurements under laboratory conditions described in [15]. The most important test procedures are:

- 10.2 (standard test conditions in laboratory),
- 10.5 (outdoor measurement of nominal operating cell temperature) and
- 10.6 (outdoor performance measurement at NOCT)

Concerning 10.5 NOCT is defined as the equilibrium mean solar cell junction temperature within an open-rack mounted module in the following standard reference environment (SRE): open rack mounted PV modules with optimised inclination at normal incidence to the direct solar beam at local solar noon and a total irradiance of 800 W/m^{2}at ambient temperature of 20 ° C and wind speed around 1 m/s.

Measurement of NOCT for PV modules applied as BIPV components are of most interest as the negative temperature effect on the maximum power is about 0.5%/ ° C (referred to conditions at 25 °C). A number of different circumstances occur when PV modules are applied as integrated components in a building, which is far from the Standard Reference Environment as described in the [15]:

- The inclination for façade application is typically 90° and for roof applications depending on the roof construction but is seldom optimised.
- Free convection at the backside of the PV modules will not occur.

As a consequence the most notable differences are in level of irradiation and operating cell temperature. Therefore, conversion from PV module specifications at standard test conditions (25 °C, 1000 W/m^2) to BIPV applicable electric system design values is of highest priority when the integration of PV in buildings continues to emerge. All BIPV applications differ from the conditions as described above. The main differences are to be found in the convective and irradiative heat exchanges on the rear side of the PV module.

In Fig. 1, the standardized reference points are given, according to the STC and NOCT conditions. Looking more in detail to this graph, one may conclude that building integrated PV applications are situated above the NOCT line. Designers and architects therefore need to calculate with extrapolated data from PV industry supplied specifications. In reality the performance behaviour of a PV module is not following a straight line but more a cloud of measurement points due to convective and irradiative energy flows that are strongly dependent on the wind and boundary conditions. Fig. 2 gives measurements of a full sunny day from four modules installed

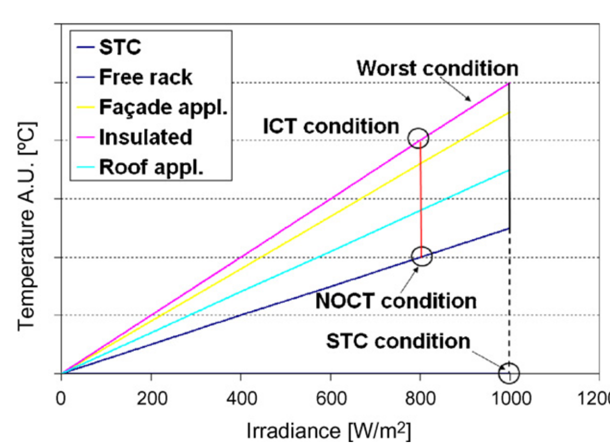

Fig. 1. Temperature difference vs. irradiance. Standardised reference points.

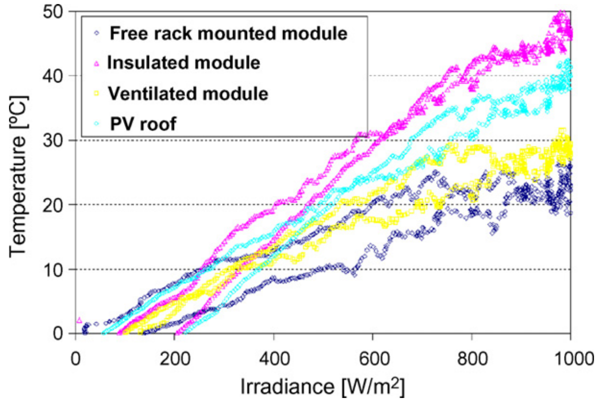

Fig. 2. Temperature difference vs. irradiance. Measurements recorded the 26th of March 2002, from four modules installed under different conditions.

under four different conditions: free rack mounting, ventilated roof, an integrated roof and a fully insulated PV module. The graph shows a plot of the temperature difference between PV-module and ambient temperature versus solar radiation.

6.3. Experimental setup

The size of the PV test reference module is derived from commonly accepted sizes in the glass industrial research, 120 cm × 120 cm. The data used for the here presented case study comes from a PV module that is composed of 121 glass-glass polycrystalline Si based cells. Fig. 3 shows a picture of the front view of the module mounted in the test reference environment (TRE). Below is giving only an outline of the experimental setup and the sensors; for a detailed description [16] is referred to.

The test reference environment is designed for testing PV modules under specific conditions under which the modules can be applied when integrated as a cladding device into the building environment. The test environment is constructed in such a way that the thermal energy obtained by convection and radiation exchanges at the rear of the PV module can be measured accurately. As indicated in Fig. 4 the test environment box is composed of an insulated cavity of 10 cm with an air inlet and outlet placed at the back of the box. Considering the long wave radiative transfer it was decided to have the cavity painted in defined colours. The box is equipped with a number of air and surface temperature sensors, making data available for modelling work.

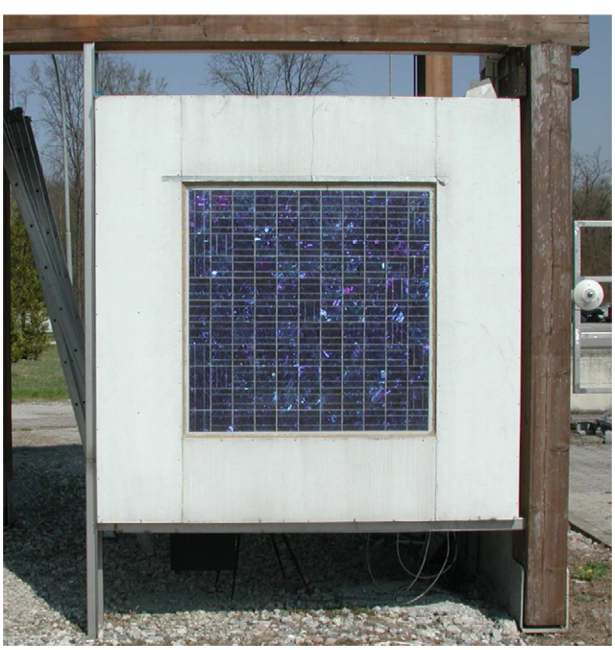

Fig. 3. Front view of the PV module.

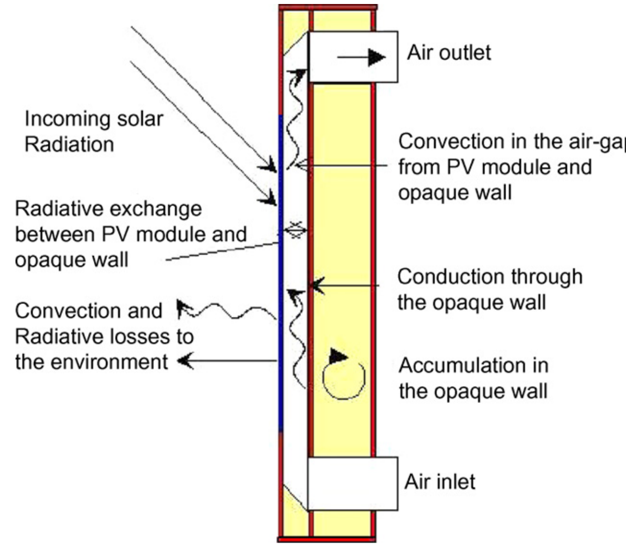

Fig. 4. View of vertical cross section. The main sources for energy transfer are indicated.

6.4. Data

The data is collected with a one minute interval on August 16th, 2002 from 00:00 to 23:59. The ventilated air-flow in the gap behind the PV module is set to a constant flow of 78.2 l/s. Table 1 shows a list of the data used in the present modelling work.

The air flow is measured by the Swema's Swemair 300 instrument based in a hot wire anemometer. It should be noted that the mean radiant temperature was not measured.

6.5. Energy transfer

In the subsequent sections we shall consider the temperature of the PV module as a state variable in the dynamical models. The background is that the efficiency of the PV element depends on a negative temperature effect of about 0.5%/ ° C on the maximum power.

The energy transfer related to the PV module has the following contributions:

- Absorption of vertical solar radiation:

$\alpha(W)AI_v$

Table 1
Data

Signal	Symbol	Units	Comments
Time	t	min	
Wind speed	W	m/s	Measured at the test site
Ambient air temperature	T_a	°C	Measured by type T thermocouples
Wood temperature	T_w	°C	Temperature backside cavity (middle). Measured by type T thermocouples
Temperature difference	ΔT	°C	Temperature difference between inlet and outlet of cavity measured by thermopile
Irradiance	I_v	W/m^2	Global irradiance on PV module measured by a CM11 pyranometer near the test site
Temperature module	T_m	°C	Measured average module temperature— calculated as average of top and bottom. Type T thermocouples are used

- Infrared radiation to the surroundings:

$\sigma\epsilon_{pv1}A(T^4 - T_{rad}^4)$

- Convection to the ambient:

$h_c(W)A(T - T_a)$

- Infrared radiation to the wood wall:

$\sigma\left(\frac{1}{\epsilon_{pv2}} + \frac{1}{\epsilon_w} - 1\right)^{-1} A(T^4 - T_w^4)$

- Convection from the PV module to the air gap:

$pw_{gap}S\rho c_p \Delta T$

Note $\alpha(W)$ and $h_c(W)$ might depend on the wind speed W.

6.6. Models

Linear and non-linear models assuming different usual simplifications for these heat contributions, have been considered in the following. In all these models, k_i parameters grouping products of physical parameters, have been introduced to simplify notation.

6.6.1. Linear model

In order to obtain the linear model we assume linearization in the heat interchange for the external surface of the PV module, and in the radiative transfer between the internal part of the PV module and the wood. As the state variable the true temperature of the module (T) is introduced.

The linear state space model describing the dynamics of the temperature of the module is

$$dT = k_1(T_a - T)\,dt + k_3\Delta T\,dt + k_4(T_w - T)\,dt + k_5 I_v\,dt + dw \quad (44)$$

$$T_m = T + e \quad (45)$$

where (44) and (45) are the system and observation equation, respectively. This model will be labelled model no. 0.

6.6.2. Non-linear models

6.6.2.1. Model with wind speed dependency. As a first extension of the linear model we will assume that the main heat exchange between the ambient and the external surface of the PV module is due to convection, and that the heat convection coefficient depends on the wind speed as described in the following non-linear state space model

$$dT = k_1 W^{k_2}(T_a - T)\,dt + k_3\Delta T\,dt + k_4(T_w - T)\,dt + k_5 I_v\,dt + dw \quad (46)$$

$$T_m = T + e \quad (47)$$

This model will be labelled model no. 1.

6.6.2.2. Model including long wave radiation. The heat convection coefficient depends on the wind speed as in the previous model no. 1. Next, a more correct description of the radiative transfer is introduced. We will assume that the long wave radiation to the surroundings are relative to some mean radiant temperature (T_{rad}). In the model, the mean radiant temperature is treated as a parameter. Furthermore, we will introduce a non-linear description of the radiative transfer between the PV module and the back-panel of wood. Finally it is also assumed that the absorptivity depends on the wind speed. The model (labelled model no. 2) is

$$dT = k_0(T_{rad}^4 - T^4)\,dt + k_1 W^{k_2}(T_a - T)\,dt + k_3\Delta T\,dt + k_4(T_w^4 - T^4)\,dt + k_5 W^{k_6} I_v\,dt + dw \quad (48)$$

$$T_m = T + e \quad (49)$$

Note that the absolute temperature now has to be used.

6.7. Results

The residuals of all the models considered are shown in Fig. 5. The standard deviation and average of the residuals, i.e. the one-step prediction error for all the models, are found in Table 2.

An important point in dynamic modelling which is often overlooked is to test the sufficiency of the model by using statistical methods. Such tests can be used to judge whether the model describes all the observed dynamics in the data. The idea is that if the given model is correct then the residuals from the estimation procedure should be serially uncorrelated, i.e. the residuals should behave as white noise.

Most often test for white noise is conducted by considering the estimated autocorrelation for the residuals. The estimated autocorrelation function for all models are seen in Fig. 6. Confidence bands of approximately 95% under the hypothesis that the residuals are white noise are also shown.

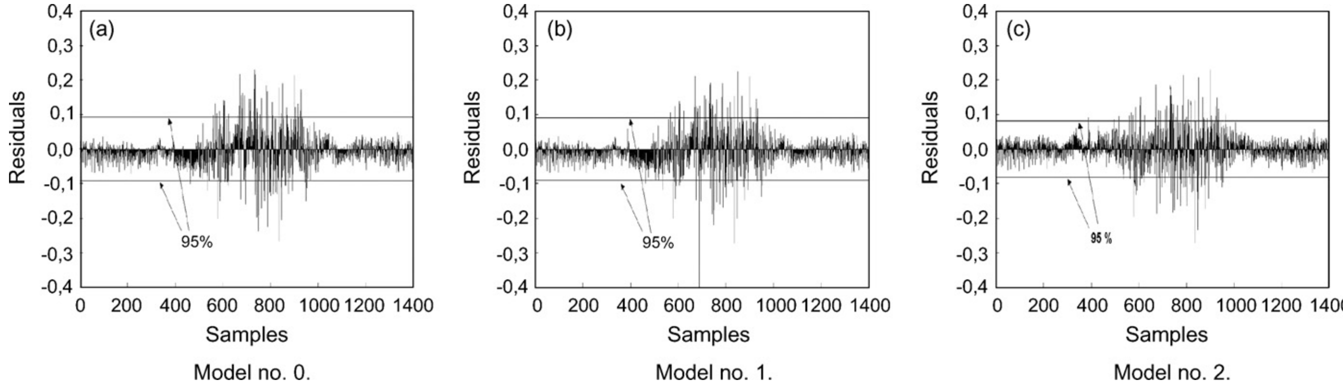

Fig. 5. Residuals for the various models.

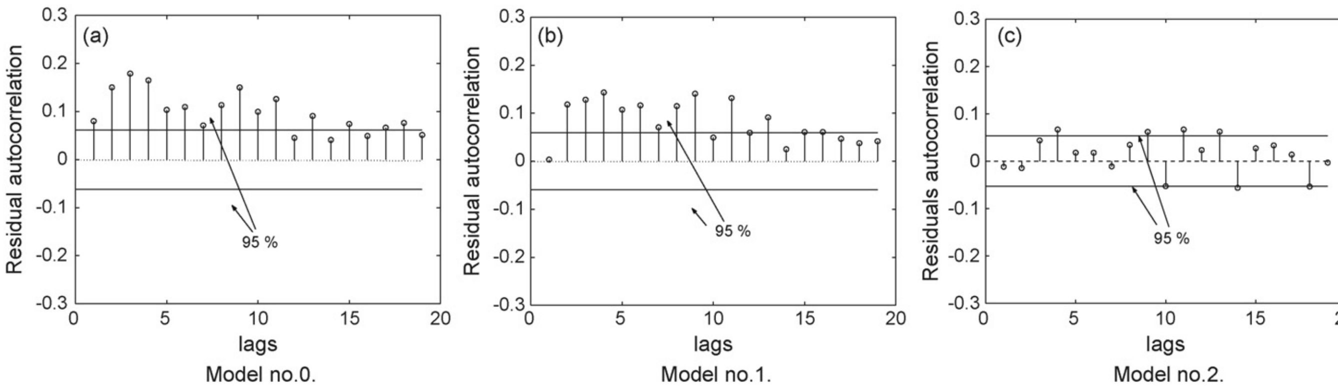

Fig. 6. Estimated autocorrelation functions for the residuals. The horizontal lines are the 95% confidence intervals for white noise tests.

If the residuals contain periodicities, a study of the correlation in the frequency domain can be more useful to reveal such periodicities than the autocorrelation function. The periodogram shows how the variation of the residuals is distributed on frequencies. For white noise this variation is equally distributed, i.e. the cumulative periodogram is a straight line from $(0, 0)$ to $(0.5, 1)$. Fig. 7 shows the estimated cumulative periodogram for all three models. In the figure is also shown confidence bands of approximately 95% under the hypothesis that the residuals are white noise.

Let us first summarize the results for the individual models:

Model 0 : This model is a linear model. It gives good predictions in a wide range of frequencies, but it has bad performance for low frequencies. Also according to the autocorrelation function of the residuals the model is not adequate.

Model 1 : This model is a simple non-linear model; only taking into account the wind speed dependency in heat convection coefficient. This model represents some improvements to the linear model as far as it is valid in a wider range of frequencies. The estimated autocorrelations for the residuals are lower than for model no. 0; but still many of the values are significantly different from zero. Considering the cumulated periodogram it is seen that the model is still not able to provide an adequate description of the low

Table 2
Standard deviation and average of residuals

Model no.	S.D.	Average
No. 0	0.0465	−0.00825
No. 1	0.0452	−0.00851
No. 2	0.0405	−0.00007

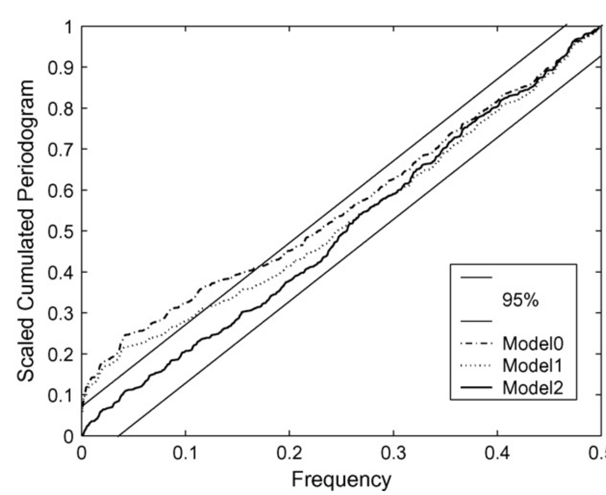

Fig. 7. Cumulated periodogram of the residuals, and corresponding confidence bands of approximately 95% for white noise tests. The unit on the frequency scale is min^{-1}.

Table 3
Maximum likelihood estimates with standard deviation of the estimates

Parameter	Estimate	S.D.
$\hat{T}_{rad}$	11.2	1.0
$\hat{k}_0$	7.28×10^{-13}	0.87×10^{-13}
$\hat{k}_1$	7.15×10^{-4}	0.42×10^{-4}
$\hat{k}_2$	0.172	0.019
$\hat{k}_3$	3.27×10^{-4}	0.87×10^{-4}
$\hat{k}_4$	1.48×10^{-12}	0.14×10^{-12}
$\hat{k}_5$	3.37×10^{-5}	0.03×10^{-5}
$\hat{k}_6$	0.0534	0.0086

$\hat{T}_{rad}$ is given in °C, and $\hat{k}_i$ are in the international system.

frequencies. In conclusion the model is still not fully adequate.

Model 2 : This is a more detailed non-linear model considering the mean radiant temperature. It presents good performance for all range of frequencies and particularly it could be used to estimate the steady state parameters. The estimated autocorrelations are very small and mostly insignificant, since all of them are within or near the 95% confidence limits. In conclusion the model seems to be adequate.

At the first hand the plot of the residuals for all the models looks very similar. However, considering the standard deviation of the errors it is seen that the simple non-linear model and the linear models have approximately the same performance; but the extended non-linear model is significantly better. It is also seen that the mean of all the errors is much smaller for the extended non-linear model. The cumulated periodogram for the residuals also clearly shows that only model no. 2 shows good steady state performance.

The obtained parameter estimates for model no. 2 are shown in Table 3 together with the corresponding approximate standard deviation of the parameter estimates. All the estimated parameters are strongly significant, and no serious correlations where observed between them.

7. Discussion

The method presented in this paper is very useful for modelling non-linear stochastic systems. The continuous time formulation allows for a direct use of prior physical knowledge as example the well known physical laws for heat transfer used in the case study. The considered case study also demonstrates that more conventional linear modelling leads to an insufficient model, whereas, the simple non-linear model based on well-known equations for heat transfer turns out to provide an adequate description of the data. Although the case study clearly demonstrated the power of the proposed method it is also clear that more measurements are needed in order to estimate the physical parameters directly. This will be the main purpose of a subsequent paper.

Process noise due to random variations or model approximations, unmodelled inputs and other model deficiencies is almost unavoidable in practice, so for most practical model building it is the recommendation of the authors to use stochastic models in describing variations in data. Furthermore, it is a clear recommendation to use PE estimation, like the maximum likelihood method, instead of OE estimation (i.e., a minimization of the simulation errors). The use of PE estimation enables the use of powerful statistical approaches for model validation as illustrated in this paper. Furthermore, the use of PE estimation allows for the total noise to be separated and quantified through the parameters of the diffusion term. These parameters can then be used for indicating deficiencies of the model in order to subsequently reveal their structural origin [6].

A parameter estimation scheme for non-linear models similar to the one presented in this paper has previously been presented by [17], who also presented an associated computer program, which has subsequently been developed into an extensive tool for identification of continuous time models called MoCaVa [18]. There are, however, a number of important differences between the estimation scheme presented here and the one implemented in MoCaVa, which essentially make the latter equivalent to an OE estimation method [10].

8. Conclusion

A method for identifying non-linear continuous–discrete time stochastic state space models has been suggested. This approach is seen as an extension to the work described in [7] where only linear models are considered.

The continuous–discrete stochastic state space models have been advocated for modelling dynamic systems in continuous time using discrete time data, because such models have several attractive features. First of all the approach allows setting up non-linear models using well-known physical laws for the heat transfer and subsequently the parameters are estimated using efficient statistical methods. It is the intention by the proposed modelling method to try to fill the gap between a detailed deterministic physical modelling approach based solely on physical prior knowledge, and the opposite approach where rather simple (typically linear) relation is identified using a statistical (black box) approach. The combined modelling scheme is often called a grey box approach [18,13].

In particular, the prediction error decomposition (PED) provided by models of this type facilitates estimation of unknown parameters in a prediction error (PE) setting, which gives less biased and more reproducible results in the presence of significant process noise than estimation in a standard output error (OE) setting. A software implementation of the suggested PE estimation scheme is briefly presented.

A case study concerning the modelling of a PV reference component has been considered. A non-linear model has been found the most appropriate to describe the system. This model presents noticeable improvements compared to the classical linear approach. The selected output in this case is the temperature of the PV component which is important as far as it highly influences the electrical efficiency of the component. The main problem with the considered case study was that it was not possible to estimate the physical parameters and the steady state parameters directly. In order to do so more measurements are needed, and this will be addressed in a subsequent study.

References

[1] A.H. Jazwinski, Stochastic Processes and Filtering Theory, Academic Press, New York, USA, 1970.

[2] K.J. Åström, Introduction to Stochastic Control Theory, Academic Press, New York, USA, 1970.

[3] J.N. Nielsen, H. Madsen, P.C. Young, Parameter estimation in stochastic differential equations: an overview, Annual Reviews in Control 24 (2000) 83–94.

[4] H. Unbehauen, G.P. Rao, Continuous-time approaches to system identification—a survey, Automatica 26 (1) (1990) 23–35.

[5] H. Unbehauen, G.P. Rao, A review of identification in continuous-time systems, Annual Reviews in Control 22 (1998) 145–171.

[6] N.R. Kristensen, H. Madsen, S.B. Jørgensen, A method for systematic improvement of stochastic grey-box models, Computers and Chemical Engineering 28 (8) (2004) 1431–1449.

[7] H. Madsen, J. Holst, Estimation of continuous-time models for the heat dynamics of a building, Energy and Buildings 22 (1995) 67–79.

[8] M.J. Jiménez, H. Madsen, K.K. Andersen, How to get physical parameters using Matlab, in: Proceedings of the International Conference on Dynamic Analysis and Modelling Techniques. Organised by PASLINK EEIG and JRC. Ispra, Italy, 13 and 14 November 2003, EUR 21187, ISBN 92-894-7794-6, 2004.

[9] K. Andersen, H. Madsen, L. Hansen, Modelling the head dynamics of a building using stochastic differential equations, Energy and Buildings 31 (2000) 13–24.

[10] N.R. Kristensen, H. Madsen, S.B. Jørgensen, Parameter estimation in stochastic grey-box models, Automatica 40 (2) (2004) 225–237.

[11] N.R. Kristensen, H. Madsen, Continuous Time Stochastic Modelling – CTSM 2. 2 – Mathematics Guide, Technical University of Denmark, Lyngby, Denmark, 2003.

[12] H. Madsen, J. Holst, Modeling Nonlinear and Nonstationary Time Series, IMM, Technical University of Denmark, Lyngby, Denmark, 2000.

[13] J. Holst, U. Holst, H. Madsen, H. Melgaard, Validation of grey box models, in: L. Dugard, M. M'Saad, I.D. Landau (Eds.), Selected Papers from the 4th IFAC Symposium on Adaptive Systems in Control and Signal Processing, Pergamon Press, 1992, pp. 407–414.

[14] L. Ljung, System Identification: Theory for the User, 2nd ed., Prentice-Hall, Upper Saddle River, USA, 1999.

[15] IEC 61215, Crystalline silicon terrestrial photovoltaic (PV) modules—design qualification and type approval (2005).

[16] J.J. Bloem. BIPV case study for modelling and analysis. in: Proceedings of the International Conference on Dynamic Analysis and Modelling Techniques. Organised by PASLINK EEIG and JRC. Ispra, Italy, 13 and 14 November 2003. EUR 21187, ISBN 92-894-7794-6, 2004.

[17] T. Bohlin, S.F. Graebe, Issues in nonlinear stochastic grey-box identification, International Journal of Adaptive Control and Signal Processing 9 (1995) 465–490.

[18] T. Bohlin, A grey-box process identification tool: theory and practice, Tech. Re IR-S3-REG-0103, Department of Signals, Sensors and Systems, Royal Institute of Technology, Stockholm, Sweden (2001).